THE JOURNAL OF BIOLOGICAL CHEMISTRY VOL. 281, NO. 18, pp. 12596–12602, May 5, 2006

Thermodynamic Analysis Reveals Structural Rearrangement during the Acylation Step in Human Trypsin 4 on 4-Methylumbelliferyl 4-Guanidinobenzoate Substrate Analogue*

Received for publication, November 16, 2005, and in revised form, February 8, 2006 Published, JBC Papers in Press, February 21, 2006, DOI 10.1074/jbc.M512301200

Júlia Tóth, Linda Gombos, Zoltán Simon, Péter Medveczky, László Szilágyi, László Gráf, and András Málnási-Csizmadia[1]

From the Department of Biochemistry, Eötvös Loránd University, Pázmány Péter sétány 1/C, H-1117 Budapest, Hungary

Human trypsin 4 is an unconventional serine protease that possesses an arginine at position 193 in place of the highly conserved glycine. Although this single amino acid substitution does not affect steady-state activity on small synthetic substrates, it has dramatic effects on zymogen activation, interaction with canonical inhibitors, and substrate specificity toward macromolecular substrates. To study the effect of a non-glycine residue at position 193 on the mechanism of the individual enzymatic reaction steps, we expressed wild type human trypsin 4 and its R193G mutant. 4-Methylumbelliferyl 4-guanidinobenzoate has been chosen as a substrate analogue, where deacylation is rate-limiting, and transient kinetic methods were used to monitor the reactions. This experimental system allows for the separation of the individual reaction steps during substrate hydrolysis and the determination of their rate constants dependably. We suggest a refined model for the reaction mechanism, in which acylation is preceded by the reversible formation of the first tetrahedral intermediate. Furthermore, the thermodynamics of these steps were also investigated. The formation of the first tetrahedral intermediate is highly exothermic and accompanied by a large entropy decrease for the wild type enzyme, whereas the signs of the enthalpy and entropy changes are opposite and smaller for the R193G mutant. This difference in the energetic profiles indicates much more extended structural and/or dynamic rearrangements in the equilibrium step of the first tetrahedral intermediate formation in wild type human trypsin 4 than in the R193G mutant enzyme, which may contribute to the biological function of this protease.

Trypsin is a prototype of the S1 serine protease family, the largest group of proteases. The residues indispensable for its enzymatic activity, His-57, Asp-102, and Ser-195 (chymotrypsinogen numbering), are structurally conserved and are referred to collectively as the catalytic triad (1). These residues are located at the active site of the enzyme. As the first step of the catalytic cycle, the enzyme binds the substrate forming the non-covalent Michaelis complex. The hydroxyl oxygen of the catalytic serine makes a nucleophilic attack on the electron-deficient carbonyl carbon of the scissile bond, and a covalent bond is formed. The attacked carbon atom becomes tetrahedrally coordinated; thus this state is called the first tetrahedral intermediate. In the next step, this species breaks down to yield the C-terminal (first) product and the acyl-enzyme. The acylation is followed by deacylation, a mechanistically similar action, in which the acyl-ester bond is attacked by a water molecule that has previously been activated by His-57 (2, 3).

During the hydrolysis of the scissile bond, tetrahedral intermediates are developed that are stabilized via hydrogen bonding interactions, in which the amido groups of residues Gly-193 and Ser-195 act as H-donors and the developing oxyanion intermediate is the acceptor (4, 5). Despite glycine being the far most convenient amino acid at position 193 for optimal transition state stabilization, rare examples are known in which this site is occupied by a non-glycine residue. The best characterized such enzyme is mesotrypsinogen (6, 7) and its alternatively spliced variant, human trypsinogen 4 (8, 9), in which an arginine can be found at position 193 (Fig. 1). Human trypsin 4 has recently been shown to selectively process myelin basic protein *in vitro*, the most abundant membrane protein in the central nervous system (10). Upon proteolytic cleavage, it generates a peptide fragment comprising the sequence that is recognized by major antibodies found in patients with multiple sclerosis. These results suggest that human trypsin 4 may be one of the candidate proteases involved in the pathomechanism of this neurodegenerative disease.

Other instances also exist when the non-glycine-possessing enzymes at position 193 are not to be considered as mutant proteins, but these variants represent the native enzymes; *Trimeresurus stejnejeri* plasminogen activator (11) and *Dermasterias imbricata* trypsin 1 (12) belong to this group of site 193 variants. Naturally occurring 193 mutants are reported among coagulation factors, including Factor XI (13), Factor IX (14), and Factor VII as well (15). These enzymes were characterized biochemically and found to be altered in various aspects when compared with their Gly-193-possessing counterpart. Deficiency of autoactivation and impaired activation of other zymogens (16, 17), low coagulant activity in the case of blood coagulation factors, cleavage of canonical inhibitors instead of being inhibited (12, 18), and reduced rate along with restricted substrate specificity toward macromolecular substrates have been reported. These observations and structural data (human trypsin 4, Protein Data Bank code: 1h4w (19)) together indicate that the interaction with their respective protein partners is hindered by steric clashes and/or electrostatic repulsions upon binding to them due to the bulky and/or charged side chain at position 193 (S2′ subsite according to the Schechter-Berger nomenclature (20)). The R193G variant human trypsin 4 shows practically identical catalytic properties and sensitivity to canonical inhibitors as human trypsin 1 (16). Our recent results confirm this finding. The k_{cat} on Z-GPR-pNA substrate increased ~3-fold, and the K_m increased 2–3-fold; thus the k_{cat}/K_m value did not change significantly upon the substitution of Gly-193 with

* This work was supported by Hungarian Scientific Research Fund Grants OTKA T037568 (to L. S.) and TS49812 and T047154 (to L. G.) and by a European Molecular Biology Organization (EMBO), EMBO Howard Hughes Medical Institute awards, a Békéssy fellowship, and Wellcome Trust International Research and Development Award Scheme, National Office for Research and Technology RET 14/2005 (to A. M-C.).
[1] To whom correspondence should be addressed. Tel.: 36-1-381-2171; Fax: 36-1-381-2172; E-mail: amc26@le.ac.uk.

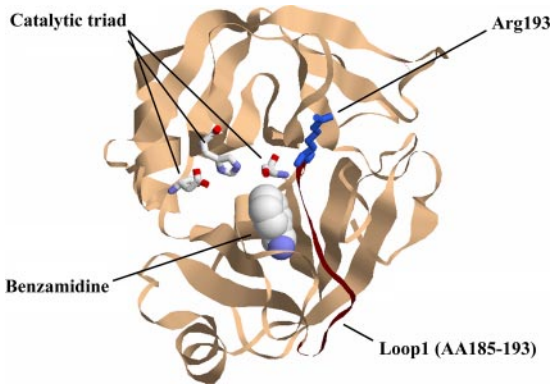

FIGURE 1. **Three-dimensional structure of wild type human trypsin 4 based on the Protein Data Bank file 1h4w visualized using software RasTop.** Residues His-57, Asp-102, and Ser-195, comprising the catalytic triad, are displayed along with Arg-193 located in the C terminus of Loop1 and the benzamidine molecule in the substrate binding pocket. *AA*, amino acids.

arginine (21). The equilibrium dissociation constants of wild type human trypsin 4 toward canonical inhibitors increased 2–3 orders of magnitude when compared with the pancreatic isoform human trypsin 1. These altered kinetic parameters were restored upon the back mutation of Arg-193 to glycine. Based on these data, the R193G mutant human trypsin 4 can be considered as a model for the pancreatic trypsin isoform. Another effect of a non-glycine residue at position 193 is that the geometry of the 192–193 peptide bond is assumed to be distorted; thus the structure of the S1 binding site and the oxyanion hole are perturbed in the active enzyme (22). Another study on the structural and energetic consequences of the amino acid substitution at position 193 with a non-glycine residue in thrombin and in rat trypsin has been reported recently (23). From kinetic and structural data, it has been deduced that Gly-193 contributes to substrate binding by the stabilization of both the ground and the transition states despite the lack of a drastic structural perturbation even in the G193P mutant.

Although human trypsin 4 has been comprehensively characterized and diverse aspects have been examined, thermodynamic consequences of replacing the conserved glycine 193 with arginine on substrate hydrolysis are presently unknown in this enzyme. The aim of this work was to identify the enzymatic steps that are affected by the substitution of glycine with arginine at position 193 in human trypsin 4. Furthermore, we intended to shed light on the differences in the thermodynamics of substrate hydrolysis for the wild type and the R193G mutant[2] enzyme. In the present study, reactions of wild type and R193G mutant human trypsin 4 on 4-methylumbelliferyl 4-guanidinobenzoate (MUGB)[3] fluorogenic substrate analogue were followed using a stopped flow apparatus. This substrate is convenient for the present study as it is known that deacylation is slower for MUGB than the acylation step, and the final reaction step being the rate-limiting event is the requisite for the unambiguous determination of the rate constants of all preceding steps. On the grounds of our kinetic data, we propose a refined model for the reaction of human trypsin 4 and its R193G mutant on MUGB substrate, where the acylation step can be kinetically separated from the preceding reversible step. We assign this event as the formation of the first tetrahedral intermediate. Thermodynamic analysis of the acylation process revealed a marked difference between these enzymes; formation of the first tetrahedral intermediate is highly exothermic and accompanied by a large entropy decrease for the wild type enzyme. In contrast, it is endothermic accompanied by entropy gain for the R193G mutant. We conclude that along the first stage of acylation, wild type human trypsin 4 passes through significant structural and/or dynamic conversions, whereas a different rearrangement occurs in the R193G mutant enzyme.

[2] Denomination of these enzymes might be confusing as the default amino acid at position 193 is glycine in serine proteases. Still, the arginine-possessing human trypsin 4 is a naturally occurring isoform and therefore designated as the wild type enzyme. The R193G variant might be termed a back mutant or revertant referring to the otherwise conserved glycine at this position.

[3] The abbreviations used are: MUGB, 4-methylumbelliferyl 4-guanidinobenzoate; MU, methylumbelliferone; $hTry4_{WT}$, wild type human trypsin 4; $hTry4_{R193G}$, R193G mutant human trypsin 4; TI_1, first tetrahedral intermediate; Tricine, *N*-[2-hydroxy-1,1-bis(hydroxymethyl)ethyl]glycine.

EXPERIMENTAL PROCEDURES

Reagents—4-methylumbelliferyl 4-guanidinobenzoate and porcine enterokinase was purchased from Sigma. Isopropyl-beta-D-thiogalactopyranoside was purchased from Fermentas. Benzamidine-Sepharose™ 4 Fast Flow column was obtained from Amersham Biosciences. All other materials were of reagent grade and were obtained from various suppliers.

Cloning and Expression of Human Trypsinogen 4 and Its Variants—Wild type human trypsinogen 4 was cloned as described previously (19). The mutation R193G was introduced by the megaprimer PCR mutagenesis method using the following mutant oligonucleotide primer: $hTry4_{R193G}$ 5′-TCC TGC CAG GGT GAC TCC GGT GGC-3′ (Invitrogen). The inactive human trypsin 4 mutant, in which Ser-195 of the catalytic triad is replaced by alanine, was generated with the same method using the following oligonucleotide: $hTry4_{S195A}$ 5′-CCT GCC AGC GTG ACG CTG GTG GCC CTG TG-3′. PCR products were cloned into the modified pET-17b vector (19). Proteins were expressed and refolded as described previously (17). The correct fold and disulfide bond arrangement of the zymogen was checked by SDS-PAGE under reducing and non-reducing conditions. Trypsinogen was activated by adding porcine enterokinase (1:1000 molar ratio) in 50 mM Tris-HCl, pH 8.0, 100 mM NaCl, 10 mM $CaCl_2$ followed by affinity purification on a benzamidine-Sepharose column and eluted with 10 mM HCl. Protein containing fractions were pooled, concentrated by ultrafiltration using a Centricon filter unit (Amicon) and kept in aliquots at −20 °C. Protein concentration was determined from absorption data calculated with the theoretical extinction coefficient $\epsilon_{280} = 40570\ M^{-1}\ cm^{-1}$. Purity was assessed by 15% SDS-PAGE using the Laemmli buffer system (24).

Transient Kinetic Measurements—Stopped-flow transients were recorded on a KinTek SF-2004 instrument (KinTek Corp.) using a 450-watt Hg-Xe super-quiet lamp (Hamamatsu Corp.). Excitation wavelength was 365 nm with a bandwidth of 0.5 nm, and a WG420 nm cut-off filter (Comar Instruments) was used on the emission side. 8 ml/sec flow rate was applied, and sample volumes were 40 μl with a mixing ratio of 1:1. Fluorescence emission intensities were measured with a photomultiplier set to 700 V voltage. The dead time of the stopped flow apparatus is 1.0 ms. For the substrate saturation studies, 0.1 μM enzyme was mixed with 0.94–500 μM 4-methylumbelliferyl 4-guanidinobenzoate substrate analogue for the wild type and 0.94–200 μM substrate for the R193G mutant human trypsin 4 (concentrations are stated as final values in the reaction chamber). Buffer conditions were 20 mM Tricine, 10 mM $CaCl_2$, pH 8.0, at 20.0 °C. Data were collected on a logarithmic time base to ensure that a significant number of data points were recorded even for a multiphase process. The analyzed transients are averages of 4–7 recorded traces.

To obtain information on the thermodynamic properties of the reaction, 0.1 μM enzyme was mixed with saturating concentrations of substrate (500 μM for wild type and 200 μM for the R193G mutant enzyme), and the reaction was monitored in 3 °C increments over the temperature range of 6–36 °C. Buffer conditions were 20 mM Tricine, 10 mM

$CaCl_2$, pH 8.0 ± 0.1. Using the correlation $\Delta pK_a/10\,°C = -0.21$ for Tricine, the pH was adjusted at room temperature to 7.6–8.2 to give the value of 8.0 ± 0.1 at different experimental temperatures.

Kinetic and Thermodynamic Analysis—Reaction profiles were analyzed by fitting to double exponential functions using the KinTek software (KinTek Corp.) and OriginLab v7.5 (MicroCal Software). Data were corrected for spontaneous hydrolysis of the substrate, which proved to be significant at higher temperatures. Derivation of the individual rate constants is described under "Results." Activation parameters were calculated from the linear plots of ln (k/T) *versus* $1/T$ according to Equation 1 (25), where k is the rate constant, R is the gas constant (8.314 $Jmol^{-1}\,K^{-1}$), T is the absolute temperature, N_A is Avogadro's number, h is Planck's constant, the enthalpy of activation $\Delta H^{\ddagger} = -\text{slope} \times 8.314\ Jmol^{-1}$, and the entropy of activation $\Delta S^{\ddagger} = (\text{intercept} - 23.76) \times 8.314\ Jmol^{-1}\,K^{-1}$. The free energy of activation ($\Delta G^{\ddagger}$) was calculated using Equation 2.

$$\ln(k/T) = \ln(R/N_A h) + \Delta S^{\ddagger}/R - \Delta H^{\ddagger}/RT \qquad \text{(Eq. 1)}$$

$$\Delta G^{\ddagger} = \Delta H^{\ddagger} - T\Delta S^{\ddagger} \qquad \text{(Eq. 2)}$$

Standard free energy changes for equilibria ($\Delta G°$) were calculated from Equation 3. Standard enthalpy ($\Delta H°$) and entropy changes ($\Delta S°$) were obtained from the linearized van't Hoff plot according to Equation 4.

$$\Delta G° = -RT\ln K \qquad \text{(Eq. 3)}$$

$$\ln K = \Delta S°/R - \Delta H°/RT \qquad \text{(Eq. 4)}$$

RESULTS

Applied Model for the Reaction—Fig. 2 shows representative stopped-flow traces on mixing wild type and R193G mutant human trypsin 4 with MUGB substrate under pseudo-first order reaction conditions. The time course of fluorescence change during the reaction showed a burst phase with a subsequent linear phase for both enzymes (Fig. 2, *A–C*). Furthermore, the burst followed a double exponential with a fast and a slow observed rate constant. These observed rate constants had a hyperbolic dependence on substrate concentration (Fig. 3), indicating that the reversible substrate binding is followed by at least one further step. The fluorescent signal is generated along these subsequent steps, namely the chemical reaction. In addition, the double-phase character of the burst revealed two distinct, kinetically separable events during the hydrolysis of MUGB and indicated that the first one is a reversible step. Finally, the linear phase following the burst is the consequence of the liberation of the regenerated enzyme due to deacylation. Taking these observations together, the following schematic four-step model was assumed to describe the reactions.

$$E + S \underset{k_{-1}}{\overset{k_1}{\rightleftharpoons}} E{\cdot}S \underset{k_{-2}}{\overset{k_2}{\rightleftharpoons}} C^{*} \xrightarrow{k_3} E - P2 + P1^{*} \xrightarrow{k_4} E + P2$$

SCHEME 1

where E denotes the free enzyme, S stands for the substrate (MUGB), C is a covalent enzyme-substrate complex, P1 and P2 denote the first product (4-methylumbelliferone) and second product (guanidinobenzoate), respectively, and the species providing fluorescent signal are marked with an asterisk.

To validate the supposed mechanism, we probed whether the fluorescent signal is generated during the binding of the substrate or in subsequent reaction steps. We performed the experiments with the S195A mutant human trypsin 4, which is able to bind MUGB but cannot catalyze acylation. Upon mixing MUGB with the catalytically inactive variant enzyme (26), neither the burst nor the following linear phase could be detected. This finding indicates that predominant fluorescent signal is not generated during binding events.

A lag phase was expected to appear at the initial phase of the time courses as the signal-generating step is preceded by another step, namely the binding of the substrate. However, we failed to detect any

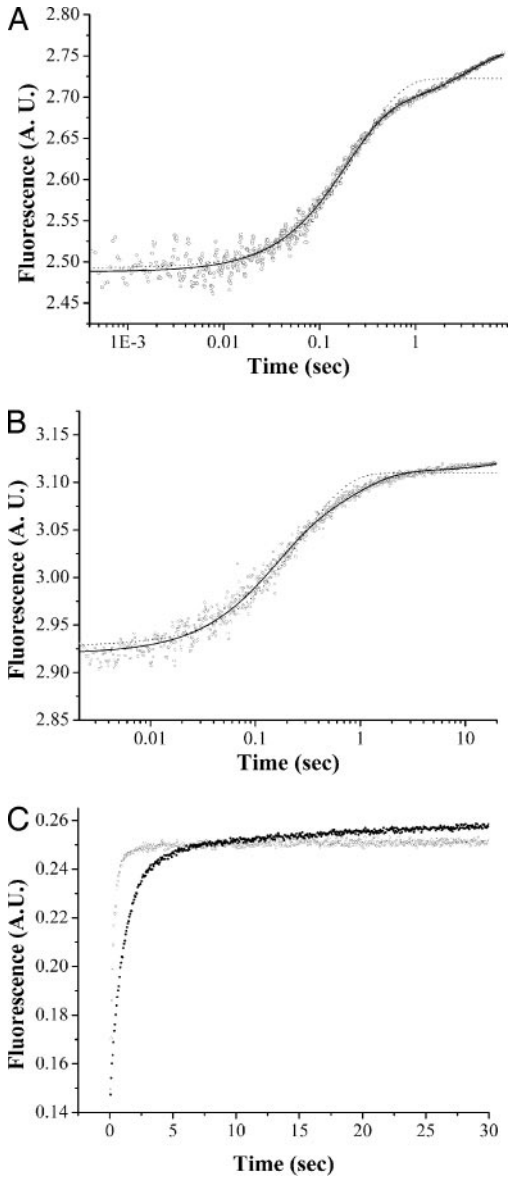

FIGURE 2. **Stopped-flow records on interaction of wild type (*A*) and R193G mutant (*B*) human trypsin 4 with 4-methylumbelliferyl 4-guanidinobenzoate ester substrate at 36 and 12 °C, respectively.** 0.1 μM wild type and R193G mutant enzymes were mixed with 60 and 200 μM concentrations of substrate, respectively, and the fluorescent emission was monitored through a 420 nm cut-off filter with 365 nm excitation. The data presented here were collected on a logarithmic time base. The analyzed curves are averages of 5–7 recorded traces. Transients could be described with double exponential functions (*solid line*) followed by a linear phase. The slope of the linear (steady-state) phases were determined in 30–100-s time base records (*e.g. panel C*) and subtracted from the recorded traces for a better visualization of the two-phase burst following the equation $F(t) = A_{fast} \times e^{-k\,obs\,fast \times t} + A_{slow} \times e^{-k\,obs\,slow \times t} + F_{\infty}$, where $F(t)$ is the fluorescence at time t, A is the amplitude, k is the observed rate constant, and F_{∞} is the final fluorescence intensity. Fitted single exponentials (*dashed line*) are presented to show the deviation of the measured data from a single-phase burst. *A. U.*, arbitrary units. *C*, single time base records on mixing 0.1 μM wild type (●) or R193G mutant enzyme (○) with 15 μM 4-methylumbelliferyl 4-guanidinobenzoate substrate analogue. Buffer conditions were 20 mM Tricine, 10 mM $CaCl_2$, pH 8.0, at 20.0 °C.

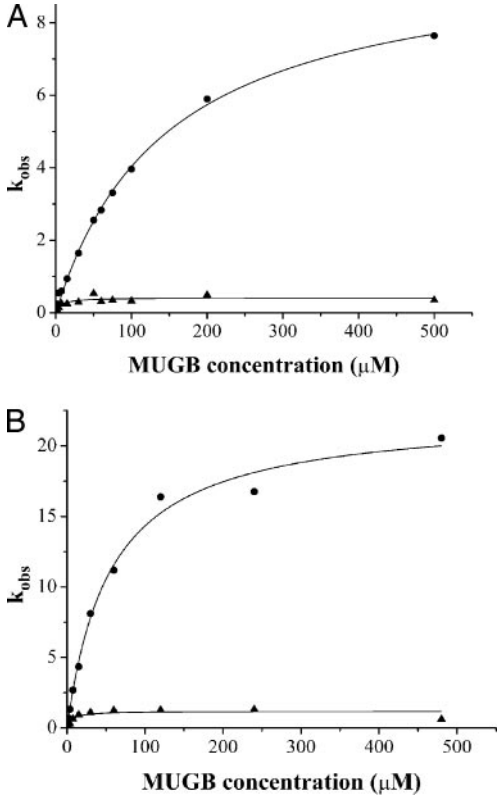

FIGURE 3. **Rate data from double exponential fits of the reaction of wild type (*A*) and R193G human trypsin 4 (*B*) on MUGB substrate, plotted against substrate concentration.** Traces could be described with a two-phase burst followed by a linear phase. Reaction profiles were analyzed by fitting to double exponential functions. Observed rate constants for the fast (●) and the slow phase (▲) of the burst are shown for the wild type (*A*) and the R193G mutant enzyme (*B*), respectively. The observed rate constants had a hyperbolic dependence on substrate concentration. Elementary rate constants were calculated using parameters of the fitted hyperbolas.

sign of a lag. A possible explanation for the lack of the lag phase is that ~5% of the total fluorescence intensity appears upon the binding of MUGB to the active site of the enzyme. This presumption was confirmed by modeling the reaction with Berkeley Madonna software, which showed that a small fluorescence intensity increase upon the binding step readily compensates the lag phase, which thus becomes undetectable. We also assumed that the fluorescence intensity of 4-methylumbelliferone does not change significantly upon dissociation from the surface of the enzyme.

The observed rate constants showed a hyperbolic dependence on substrate concentration. The plot of the observed rate constants against MUGB concentration yielded different profiles for the two enzymes (Fig. 3). The fast phase was half-saturated at about 148 μM MUGB and the maximal rate of 9.95 ± 0.4 s^{-1} for wild type human trypsin 4 and reached the value of 23.9 ± 1.4 s^{-1} with half-saturation at 58 μM substrate concentration for the R193G mutant enzyme at 20.0 °C. Linear fits to the initial part of the observed rate constant of the fast phase plotted against substrate concentration yielded an intercept of 0.23 ± 0.04 s^{-1} and an initial slope of 0.068 ± 0.0004 μM^{-1} s^{-1} for the wild type enzyme, whereas these values are 0.042 ± 0.006 s^{-1} and 0.38 ± 0.019 μM^{-1} s^{-1} for the R193G mutant. The slow phase got saturated at significantly lower substrate concentrations and had a maximal rate of 0.42 ± 0.03 s^{-1} for the wild type enzyme and 1.44 ± 0.27 s^{-1} for the glycine-possessing counterpart. Amplitude of the fast phase showed an increasing hyperbolic function, whereas the amplitude of the slow phase had a decreasing hyperbolic dependence on the substrate concentration for wild type human trypsin 4. In contrast, amplitudes of the fast and the slow phase were constant in the examined substrate concentration range for the R193G mutant. However, at saturating substrate concentrations, the fast phase is dominant for both enzymes; the relative amplitude of the fast phase comprises 95% of the total amplitude for the wild type and 85% for the R193G mutant enzyme at 20.0 °C.

TABLE 1

Kinetic parameters for the reaction of wild type and R193G mutant human trypsin 4 on MUGB substrate at 20.0 °C

Elementary rate constants (k_2, k_{-2}, k_3, k_4) and equilibrium constant of the formation of the first tetrahedral intermediate (K_2) describing the reaction of wild type and R193G mutant human trypsin 4 on 4-methylumbelliferyl 4-guanidinobenzoate substrate at 20.0 °C. 0.1 μM enzyme was mixed in a stopped-flow apparatus with increasing concentrations of substrate until saturation was reached. The fluorescence change was monitored with excitation at 365 nm and emission detected through a 420 nm cut-off filter. The transients fitted to double exponentials followed by a linear phase. Elementary rate constants were calculated using Equations 5–9 presented under "Results." Each value represents the mean and standard deviation of three and two independent data sets for the wild type and the R193G mutant enzyme, respectively, each originating from 5–7 recorded traces.

	$hTry4_{WT}$	$hTry4_{R193G}$
k_2 (s^{-1})	9.19 ± 0.01	20.22 ± 1.4
k_{-2} (s^{-1})	0.81 ± 0.05	3.56 ± 0.006
k_3 (s^{-1})	0.46 ± 0.02	1.70 ± 0.3
k_4 (s^{-1})	(1.85 ± 0.51) × 10^{-3}	(3.28 ± 3.1) × 10^{-4}
K_2	11.4 ± 0.7	5.68 ± 0.4

The ratio of amplitudes of the fast and the slow phase will be set by the equilibrium constant for the formation of the covalent enzyme-substrate complex (K_2) (K_2 = amplitude $_{\text{fast phase}}$/amplitude $_{\text{slow phase}}$). The observed rate constant of the fast phase will be a composite of the equilibrium constant and the forward rate constant of the second reaction step (k_{obs} fast phase = $k_2 \times (K_2 + 1)/K_2$), and it will also be equal to the sum of the forward and reverse rate constants for this event (k_{obs} fast phase = $k_2 + k_{-2}$) at saturating substrate concentration. Furthermore, the equilibrium dissociation constant for the substrate binding step ($K_d = k_{-1}/k_1$) is derived from the slope of the observed rate constant-substrate concentration function (k_{obs} fast phase initial slope = k_2/K_d). The observed rate constant of the slow phase will be a composite of the equilibrium constant of the second reaction step (K_2) and the rate constant of the third step (k_{obs} slow phase = $k_3 \times K_2/(K_2 + 1)$. Finally, the linear phase following the burst corresponds to the steady state; thus the rate constant of deacylation can be derived from the slope of the linear phase (k_4 = steady-state slope/(amplitude $_{\text{fast phase}}$ + amplitude $_{\text{slow phase}}$). Elementary rate constants and equilibrium constants for the individual reaction steps were calculated using Equations 5–9 presented below and are summarized in Table 1.

$$K_2 = \text{amplitude}_{\text{fast}}/\text{amplitude}_{\text{slow}} \quad \text{(Eq. 5)}$$

$$k_2 = K_2 \times k_{\text{obs fast}}/(K_2 + 1) \quad \text{(Eq. 6)}$$

$$k_{-2} = k_{\text{obs fast}} - k_2 = k_2/K_2 \quad \text{(Eq. 7)}$$

$$k_3 = k_{\text{obs slow}} \times (K_2 + 1)/K_2 \quad \text{(Eq. 8)}$$

$$k_4 = \text{steady state slope}/(\text{amplitude}_{\text{fast}} + \text{amplitude}_{\text{slow}}) \quad \text{(Eq. 9)}$$

Comparison of the Catalytic Cycle of the Wild Type and R193G Mutant Human Trypsin 4—We studied the effect of R193G substitution in human trypsin 4 on the catalytic process on 4-methylumbelliferyl 4-guanidinobenzoate substrate. Using transient kinetics, we examined which enzymatic steps and states are affected by this mutation. Data originating from the substrate saturation experi-

TABLE 2

Activation and thermodynamic parameters for the reaction of wild type and R193G human trypsin 4 on MUGB substrate

Activation and thermodynamic parameters were calculated using Equations 1–4. Values for the intercepts and slopes represent the mean and standard deviations of the fitted linear functions.

	hTry4$_{WT}$				*hTry4*$_{R193G}$			
	k_2[a]	k_{-2}[a]	K_2[b]	k_3[a]	k_2[a]	k_{-2}[a]	K_2[b]	k_3[a]
Slope	−10.9 ± 0.5	−19.9 ± 1.4	8.9 ± 1.6	−7.1 ± 1.1	−9.3 ± 0.6	−6.6 ± 0.7	−2.7 ± 0.3	−2.6 ± 1.3
Intercept	33.6 ± 1.8	61.8 ± 4.6	−28.1 ± 5.4	18.3 ± 3.9	28.5 ± 2.2	18.1 ± 2.3	10.3 ± 0.9	3.7 ± 4.4
$\Delta H^{\ddagger}$ (kJmol^{-1})	91.0	165.1		58.9	77.1	55.0		21.6
$\Delta S^{\ddagger}$ (kJmol^{-1}K^{-1})	0.08	0.32		−0.05	0.04	−0.05		−0.17
$\Delta G^{\ddagger}$ (kJmol^{-1}) at 293 K	67.0	72.5		72.1	65.7	68.8		70.5
ΔH° (kJmol^{-1})			−74.1				22.1	
ΔS° (kJmol^{-1}K^{-1})			−0.23				0.09	
ΔG° (kJmol^{-1}) at 293 K			−5.6				−3.1	

[a] Values of these parameters are derived from the Eyring plots.
[b] Values of these parameters are derived from the van't Hoff plots.

ments are presented in Table 1. The value of the equilibrium dissociation constant shows 2–3-fold difference ($K_{d\ \mathrm{hTry4WT}}$ = 136.1 ± 0.8 μM, $K_{d\ \mathrm{hTry4R193G}}$ = 53.55 ± 6.6 μM), indicating that energetically, the R193G mutation does not have a significant effect on the strength of MUGB binding ($\Delta G^{\circ}_{\mathrm{binding\ hTry4WT}}$ = −11.9 kJmol^{-1} at 293 K, $\Delta G^{\circ}_{\mathrm{binding\ hTry4R193G}}$ = −9.7 kJmol^{-1} at 293 K). The formation of the covalent enzyme-substrate complex for both enzymes proved to be reversible. The forward rate constant of this step is two times smaller ($k_{2\ \mathrm{hTry4WT}}$ = 9.19 ± 0.01 s^{-1}, $k_{2\ \mathrm{hTry4R193G}}$ = 20.22 ± 1.4 s^{-1}), and the reverse rate constant is four times more moderate for hTry4$_{WT}$ ($k_{-2\ \mathrm{hTry4WT}}$ = 0.81 ± 0.05 s^{-1}, $k_{-2\ \mathrm{hTry4R193G}}$ = 3.56 ± 0.006 s^{-1}); thus the equilibrium of the second reaction step is shifted more toward the forward direction in the wild type enzyme ($K_{2\ \mathrm{hTry4WT}}$ = 11.4 ± 0.7, $K_{2\ \mathrm{hTry4R193G}}$ = 5.68 ± 0.4). The next event is 3–4 times slower in the wild type enzyme ($k_{3\ \mathrm{hTry4WT}}$ = 0.46 ± 0.02 s^{-1}, $k_{3\ \mathrm{hTry4R193G}}$ = 1.70 ± 0.29 s^{-1}). MUGB is turned over by both enzymes. Deacylation is slightly (5–6 times) faster by hTry4$_{WT}$ than by the R193G mutant enzyme ($k_{4\ \mathrm{hTry4WT}}$ = (1.85 ± 0.51) × 10^{-3} s^{-1}, $k_{4\ \mathrm{hTry4R193G}}$ = (3.28 ± 3.06) × 10^{-4} s^{-1}).

Thermodynamic Parameters of the Second and Third Reaction Steps—To investigate the thermodynamics of substrate hydrolysis, the reaction of wild type and R193G mutant human trypsin 4 on MUGB substrate was monitored in the temperature range of 6–36 °C. The temperature dependence of the reaction rate constants and the equilibrium constant of the second reaction step (K_2) were analyzed using the linearized Eyring and van't Hoff plots (Table 2), respectively (Figs. 4 and 5).

The standard free enthalpy (ΔH°), standard entropy (ΔS°), and standard free energy (ΔG°) values were derived from the slope and intercept of the van't Hoff plot as K_2 is directly determined by the amplitude ratio of the fast and the slow phase, whereas k_{-2} is derived from K_2 (Equations 5–7). The standard free energy change of the second reversible reaction step at 293 K (ΔG°) is negative for both enzymes. It must be noted, however, that the respective van't Hoff plots are markedly different. This step of wild type human trypsin 4 is highly exothermic ($\Delta H^{\circ}_{\mathrm{hTry4WT}}$ = −74.1 kJmol^{-1}) and accompanied by a large standard entropy decrease ($\Delta S^{\circ}_{\mathrm{hTry4WT}}$ = −0.23 kJmol^{-1} K^{-1}), which maintains the reversibility of this reaction step at 293 K. In contrast, the second reaction step for R193G is endothermic ($\Delta H^{\circ}_{\mathrm{hTry4R193G}}$ = 22.1 kJmol^{-1}) and entropy-driven ($\Delta S^{\circ}_{\mathrm{hTry4R193G}}$ = 0.09 kJmol^{-1} K^{-1}). Comparing the activation parameters for the second reaction step, there is a striking difference between these enzymes (Table 2). The slope and the intercept of the Eyring plot for the reverse reaction step (k_{-2}) of wild type human trypsin 4 dramatically differs from that of the R193G mutant. Accordingly, the activation free enthalpies are $\Delta H^{\ddagger}_{-2\ \mathrm{hTry4R193G}}$ = 55.0 kJmol^{-1} and $\Delta H^{\ddagger}_{-2\ \mathrm{hTry4WT}}$ = 165.1 kJmol^{-1}, and the activation entropies are $\Delta S^{\ddagger}_{-2\ \mathrm{hTry4R193G}}$ = −0.05 kJmol^{-1} K^{-1} and $\Delta S^{\ddagger}_{-2\ \mathrm{hTry4WT}}$ = 0.32 kJmol^{-1} K^{-1}. The third reaction step (k_3) is slightly slower in hTry4$_{WT}$ than in the R193G mutant, which is reflected in minor differences in the thermodynamic parameters (Table 2).

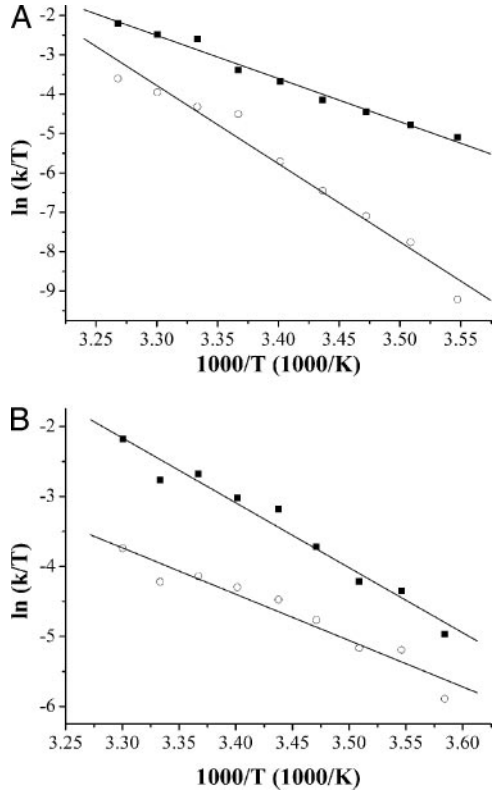

FIGURE 4. **Eyring plots for the forward (k_2) (■) and reverse rate constants of the first tetrahedral intermediate formation (k_{-2}) (○) for wild type (*A*) and R193G (*B*) human trypsin 4.** The reactions of 0.1 μM enzyme with saturating concentrations of 4-methylumbelliferyl 4-guanidinobenzoate substrate were monitored in the temperature range of 6–36 °C in 3 °C increments. Buffer conditions were 20 mM Tricine, 10 mM $CaCl_2$, pH 8.0 ± 0.1. Elementary rate constants were calculated, and ln (*k*/*T*) − values were plotted against 1000/*T*. Activation parameters were calculated from the intercept and slope of the resulting linear functions according to Equations 1–2.

DISCUSSION

We examined the effect of R193G mutation in human trypsin 4 on 4-methylumbelliferyl 4-guanidinobenzoate fluorogenic substrate using a stopped-flow apparatus. In a previous study, the structure of guanidinobenzoyl-trypsin that represents the acyl-enzyme intermediate had been reported, providing insight to the structural basis for the slow rate of deacylation (27). The guanidinobenzoyl-trypsin structure deviates markedly from the native structure in several regions, and the geometry

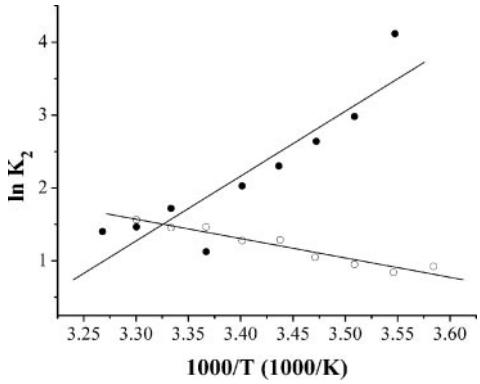

FIGURE 5. **van't Hoff plots for the equilibrium constant of the first tetrahedral intermediate formation (K_2) for wild type (●) and R193G (○) mutant human trypsin 4.** The temperature dependence of the reaction rates of 0.1 μM enzyme with saturating concentrations of 4-methylumbelliferyl 4-guanidinobenzoate substrate were measured in the temperature range of 6–36 °C in 3 °C increments. Buffer conditions were 20 mM Tricine, 10 mM $CaCl_2$, pH 8.0 ± 0.1. Elementary rate constants and equilibrium constants were calculated and ln *K* was plotted against 1000/*T*. Thermodynamic parameters were calculated from the intercept and slope of the linear fits using Equations 3–4.

around the carbonyl carbon atom of the ester bond is also distorted. As a consequence, the ordered hydrolytic water molecules in the active site of the enzyme are not close enough to the scissile ester bond to make a nucleophilic attack. The last step of the reaction mechanism, namely deacylation being rate-limiting and the use of a transient kinetic technique, together allowed reliable separation of each reaction step and determination of their rate constants.

On the basis of the substrate saturation data, we propose a refined model for the reaction of human trypsin 4 and its R193G variant on MUGB substrate. In previous studies (28, 29), the reaction of MUGB with different serine proteases was examined with steady-state kinetics, and the mechanism was determined to consist of a reversible substrate binding followed by two irreversible steps, acylation and deacylation. The use of transient kinetic techniques allowed a more detailed kinetic dissection of the process and revealed that the burst phase has a biphasic character. This phenomenon was already noted for bovine trypsin and human thrombin on 4-nitrophenyl 4-guanidinobenzoate substrate analogue having different leaving group but the same acylating moiety as MUGB (30, 31) but has not been investigated in detail. The double-phased burst indicates that following the substrate binding, a reversible and an irreversible event can be resolved. Based on the fact that MUGB binding to the S195A mutant did not cause fluorescence increase and knowing that the first released product (methylumbelliferone) is fluorescent, these two steps must be assigned between the binding and the deacylation events. Consequently, two possible explanations should be considered for these kinetically separable steps: (i) the second reversible step in the reaction mechanism is acylation, and the third irreversible step corresponds to the dissociation of the 4-methylumbelliferone from the surface of the enzyme, or (ii) the second reversible step is the formation of the first tetrahedral intermediate, and the third step is acylation, which is coupled to the fast dissociation of the leaving group from the surface of the enzyme, thus appears as an irreversible event.

The fact that tripeptide substrate analogues bearing an umbelliferyl leaving group are excellent substrates of trypsin (32) indicates that 4-methylumbelliferone must dissociate extremely fast from the surface of the enzyme and thus rules out the first theory. We suggest a refined reaction mechanism, in which substrate binding is followed by the reversible formation of the first tetrahedral intermediate, the third and irreversible event is acylation, and the final step is deacylation.

$$E + MUGB \underset{k_{-1}}{\overset{k_1}{\rightleftharpoons}} E{\cdot}MUGB \underset{k_{-2}}{\overset{k_2}{\rightleftharpoons}} E\text{-}GB\text{-}MU^* \xrightarrow{k_{3a}}$$

$$E\text{-}GB{\cdot}MU^* \xrightarrow{k_{3b}} E\text{-}GB + MU^* \xrightarrow{k_4} E + GB$$

SCHEME 2

The first action of the catalytic cycle is the reversible binding of MUGB to the substrate binding site (k_1, k_{-1}), leading to the formation of the non-covalent enzyme-substrate Michaelis complex. The binding event is followed by the nucleophilic attack of the hydroxyl group of Ser-195 on the scissile ester bond, resulting in the reversible formation of the first tetrahedral intermediate (k_2, k_{-2}). The third step is the breaking down of the tetrahedral intermediate (k_{3a}) to the first product (4-methylumbelliferone) and the acyl-enzyme (guanidinobenzoyl-trypsin). This step is highly coupled to the fast dissociation of the fluorescent group (k_{3b}), and thus it appears as an irreversible step. The final event is deacylation (k_4) by an activated water molecule when the second product (guanidinobenzoate) also departs and the enzyme regains its native conformation. The last reaction step in the mechanism leads to the recovered enzyme that can enter a forthcoming catalytic cycle.

Our data show that every step in the catalytic cycle is affected by this mutation to some extent. The K_d value decreases 3-fold in the mutant enzyme, indicating that the mutation does not change the strength of substrate binding significantly. This result is reasonable as the inhibition constant for benzamidine, a structurally similar molecule, is identical for these enzymes (21). We found that in the reaction of trypsin with MUGB, the formation of the first tetrahedral intermediate (TI_1) is reversible. The equilibrium of this reaction step is shifted more toward the forward direction at 20 °C when position 193 is occupied by an arginine instead of glycine. It must be noted, however, that the formation of TI_1 is *faster* than the acylation step for both enzymes. This is not a unique reaction mechanism among proteases. Kinetic evidence based on the acylation of chymotrypsin by specific oxygen and sulfur esters (33) as well as quantum chemical calculations (34) suggest reversible formation of TI_1. However, these studies reported rate-limiting formation of the tetrahedral intermediate followed by immediate formation of the acyl enzyme. On the other hand, a recent study on subtilisin variants (35) and another report on elastase and α-lytic protease (36) showed that breaking down of the TI_1 is rate-limiting for the hydrolytic step.

From the structure of guanidinobenzoyl-trypsin (Protein Data Bank code 1gbt (27)), it is evident that during the formation of the acyl enzyme, there is a considerable (~0.7 Å) shift in the position Ser-195 C_β toward the substrate binding cleft as the guanidinobenzoyl moiety is about 0.5 Å shorter than a P1 arginyl side chain. This movement is accompanied by several other minor distortions of the protein structure, resulting in an extremely stable acyl enzyme. We suggest that these structural rearrangements are reflected in the low value of k_3 (slow rate of acylation) and extreme stability of the acyl-enzyme complex for both enzymes. Acylation is slightly (3–4 times) slower in the wild type enzyme. The acyl-enzyme complex breaks down for both enzymes, and deacylation is slightly (5–6 times) faster by $hTry4_{WT}$ than by the R193G mutant enzyme. Due to the slower rate of formation and the faster rate of breaking down of the acyl-enzyme complex, MUGB cannot be used as an active-site titrant for wild type human trypsin 4 and presumably

neither can it be used for other serine proteases that have a non-glycine residue at position 193. As the enzyme is structurally distorted in the acyl-enzyme complex, it has to regain its native conformation during deacylation. This relaxation is faster for the wild type enzyme as it is probably advanced by greater mechanical strains that are inherently present in the protein when position 193 is occupied by an arginine when compared with the glycine-possessing enzyme.

The most important difference between the examined enzymes lies in the thermodynamics of the formation of the first tetrahedral intermediate. In a very recent study, the energetic consequence of perturbing position 193 in thrombin and in rat trypsin was reported (23). In this work, the reaction profiles were analyzed under steady-state conditions by measuring the Michaelis-Menten parameters k_{cat} and K_m, and individual rate constants were resolved from the temperature dependence of these composite functions. Contrarily, by applying transient kinetic methods, the individual reaction steps and their rate can be directly detected and separated dependably.

The energetics of the second step in the reaction mechanism was determined by the temperature dependences of the forward rate constant (k_2), the reverse rate constant (k_{-2}), and the equilibrium constant (K_2) (Figs. 4 and 5). Our data show that the equilibrium reaction of the first tetrahedral intermediate formation of R193G human trypsin 4 is an endothermic reaction and driven by a small entropy increase. These data indicate that only moderate structural and dynamic rearrangements occur during the intermediate formation of the R193G enzyme. In contrast, for the wild type enzyme, this reaction is highly exothermic and accompanied by a huge entropy decrease. In the proposed structural arrangements, the ligands and the solvent envelope might also be involved beyond the enzyme. Since thermodynamics of the forward reaction steps (k_2) for both enzymes are similar, the difference is derived mainly from the reverse reaction (k_{-2}).

The presence of arginine at position 193 may induce strain in the backbone of the active form of trypsin, which might account for the difference in the thermodynamics of the tetrahedral intermediate formation. In a previous study on Factor XIa, the crystal structure of the wild type enzyme was compared with the homology model of the G193E mutant (22). It was shown that Glu substitution can be easily accommodated at position 193 due to a slight rotation around N–C_α and C_α–C′ bonds without significant structural consequences, still perturbing the S1 binding site and the oxyanion hole. Such an argument might hold for human trypsin 4 as well. We suppose that a non-glycine residue at this position does not cause significant alterations in the structure of the active enzyme but evokes mechanical stress, which can be revealed by thermodynamic analysis. Furthermore, this presumption is indicated by our preliminary experiments in which the rate constant of the structural change from an inactive to the active conformation of wild type human trypsin 4 was smaller than that of the R193G mutant in pH-jump transient kinetic studies. Since there is a large rotation around position 193 during the pH-jump activation, the smaller rate constant indicates the presence of a structural or mechanical stress in the 192–194 backbone. It will be of interest to determine the relation between the mechanisms of the formation of the active conformation and the acylation. It was previously proposed on theoretical grounds that the "activation domain" of serine proteases might govern both zymogen activation and catalysis (37).

We conclude that extensive structural rearrangement occurs in wild type human trypsin 4 during the formation of the first tetrahedral intermediate and that new interactions are formed that restrict the dynamics of the intermediate and thus decrease entropy. The unconventional structural and kinetic properties of human trypsin 4 may contribute to the function of this enzyme in physiological and/or pathological processes in the central nervous system.

Acknowledgments—We are grateful to Dr. Mihály Kovács for valuable discussions and critical reading of the manuscript. We also thank Dr. László Polgár (Institute of Enzymology, Hungarian Academy of Sciences, Budapest) for helpful suggestions.

REFERENCES

1. Huber, R. B. W. (1978) *Acc. Chem. Res.* **11,** 114–122
2. Bender, M. L., and Kézdy, J. (1965) *Annu. Rev. Biochem.* **34,** 49–76
3. Polgár, L., and Bender, M. L. (1969) *Proc. Natl. Acad. Sci. U. S. A.* **64,** 1335–1342
4. Henderson, R. (1970) *J. Mol. Biol.* **54,** 341–354
5. Robertus, J. D., Kraut, J., Alden, R. A., and Birktoft, J. J. (1972) *Biochemistry* **11,** 4293–4303
6. Nyaruhucha, C. N., Kito, M., and Fukuoka, S. I. (1997) *J. Biol. Chem.* **272,** 10573–10578
7. Rinderknecht, H., Renner, I. G., Abramson, S. B., and Carmack, C. (1984) *Gastroenterology* **86,** 681–692
8. Rowen, L., Williams, E., Glusman, G., Linardopoulou, E., Friedman, C., Ahearn, M. E., Seto, J., Boysen, C., Qin, S., Wang, K., Kaur, A., Bloom, S., Hood, L., and Trask, B. J. (2005) *Mol. Biol. Evol.* **22,** 1712–1720
9. Wiegand, U., Corbach, S., Minn, A., Kang, J., and Muller-Hill, B. (1993) *Gene* (*Amst.*) **136,** 167–175
10. Medveczky, P., Antal, J., Patthy, A., Kékesi, K., Juhász, G., Szilágyi, L., and Gráf, L. (2006) *FEBS Lett.* **580,** 545–552
11. Zhang, Y., Wisner, A., Xiong, Y., and Bon, C. (1995) *J. Biol. Chem.* **270,** 10246–10255
12. Estell, D. A., and Laskowski, M., Jr. (1980) *Biochemistry* **19,** 124–131
13. Zivelin, A., Yatuv, R., Livnat, T., Bulvik, S., Peretz, H., Salomon, O., and Seligsohn, U. (2001) *Thromb. Haemostasis* (Suppl.) (Abstr. P1111)
14. Giannelli, F., Green, P. M., Sommer, S. S., Lillicrap, D. P., Ludwig, M., Schwaab, R., Reitsma, P. H., Goossens, M., Yoshioka, A., and Brownlee, G. G. (1994) *Nucleic Acids Res.* **22,** 3534–3546
15. Bernardi, F., Castaman, G., Pinotti, M., Ferraresi, P., Di Iasio, M. G., Lunghi, B., Rodeghiero, F., and Marchetti, G. (1996) *Hum. Mutat.* **8,** 108–115
16. Szmola, R., Kukor, Z., and Sahin-Tóth, M. (2003) *J. Biol. Chem.* **278,** 48580–48589
17. Szilágyi, L., Kénesi, E., Katona, G., Kaslik, G., Juhász, G., and Gráf, L. (2001) *J. Biol. Chem.* **276,** 24574–24580
18. Sahin-Tóth, M. (2005) *Protein Pept. Lett.* **12,** 457–464
19. Katona, G., Berglund, G. I., Hajdu, J., Gráf, L., and Szilágyi, L. (2002) *J. Mol. Biol.* **315,** 1209–1218
20. Schechter, I., and Berger, A. (1967) *Biochem. Biophys. Res. Commun.* **27,** 157–162
21. Medveczky, P., Tóth, J., Gráf, L., and Szilágyi, L. (2003) in *Protein Structure-Function Relationship* (Abbasi, A., and Ali, S. A., eds) pp. 41–53, BCC&T Press, Karachi, Pakistan
22. Schmidt, A. E., Ogawa, T., Gailani, D., and Bajaj, S. P. (2004) *J. Biol. Chem.* **279,** 29485–29492
23. Bobofchak, K. M., Pineda, A. O., Mathews, F. S., and Di Cera, E. (2005) *J. Biol. Chem.* **280,** 25644–25650
24. Laemmli, U. K. (1970) *Nature* **227,** 680–685
25. Keleti, T. (1983) *Biochem. J.* **209,** 277–280
26. Corey, D. R., and Craik, C. S. (1992) *J. Am. Chem. Soc.* **114,** 1784–1790
27. Mangel, W. F., Singer, P. T., Cyr, D. M., Umland, T. C., Toledo, D. L., Stroud, R. M., Pflugrath, J. W., and Sweet, R. M. (1990) *Biochemistry* **29,** 8351–8357
28. Urano, T., Urano, S., and Castellino, F. J. (1988) *Biochem. Biophys. Res. Commun.* **150,** 45–51
29. Payne, M. A., Neuenschwander, P. F., Johnson, A. E., and Morrissey, J. H. (1996) *Biochemistry* **35,** 7100–7106
30. Vajda, T., and Náray-Szabó, G. (1988) *Acta Biochim. Biophys. Hung.* **23,** 195–202
31. Ryan, T. J., Fenton, J. W., Chang, T., and Feinman, R. D. (1976) *Biochemistry* **15,** 1337–1341
32. Kuromizu, K., Shimokawa, Y., Abe, O., and Izumiya, N. (1985) *Anal. Biochem.* **151,** 534–539
33. Hiroara, H., Bender, M. L., and Stark, R. S. (1974) *Proc. Natl. Acad. Sci. U. S. A.* **71,** 1643–1647
34. Ishida, T., and Kato, S. (2003) *J. Am. Chem. Soc.* **125,** 12035–12048
35. Bott, R. R., Chan, G., Domingo, B., Ganshaw, G., Hsia, C. Y., Knapp, M., and Murray, C. J. (2003) *Biochemistry* **42,** 10545–10553
36. Hunkapiller, M. W., Forgac, M. D., and Richards, J. H. (1976) *Biochemistry* **15,** 5581–5588
37. Gráf, L. (1995) in *Natural Sciences and Human Thought* (Zwilling, R. ed.) pp. 139–148, Springer-Verlag, Heidelberg, Germany